International Journal of Advanced Research in Chemical Science (IJARCS)
Volume 2, Issue 3, March 2015, PP 21-32
ISSN 2349-039X (Print) & ISSN 2349-0403 (Online)
www.arcjournals.org

Photodegradation of 4-Nitrophenol in Aqueous Suspension by using new Titanium Phosphates $Li_{0.50}M_{0.25}Ti_2(PO_4)_3$ (M= Ni, Mn, and Co) Catalyzed Processes

Khadija Eddahaoui[1,2], Giuseppe Mele[1], Said Benmokhtar*[2], Iolanda Pio[1], Anna Scarlino[1]

[1]Department of Engineering for Innovation of University of Salento, via Arnesano, Lecce, Italy
[2]University Hassan II of Casablanca, Faculty of Sciences Ben M'sik, Laboratory of Chemistry and Physics of Materials, Department of Chemistry, Casablanca, Marocco.

Rachid Essehli[3],

[3]Qatar Environment and Energy Research Institute (QEERI) Bg CP4, Qatar Foundation, Doha, Qatar.

Mohamed Abdel Deyab[4]

[4]Egyptian Petroleum Research Institute (EPRI), Nasr City, Cairo, Egypt.

Abstract: *We have extended our research interest on titanium phosphates $M_{0.50}Ti_2(PO_4)_3$, with M = Mg, Mn, Fe, Co, Ni, Cu,) to titanium phosphates $Li_{0.5}M_{0.25}Ti_2(PO_4)_3$ (M= Mn, Co, Ni). Three crystal structures have been determined in rhombohedral system, space group $R\bar{3}$ (N°.167) with a ~ 8.50Å and c ~ 20.95Å.The structures, which are compared to that of $Mn_{0.50}Ti_2(PO_4)_3$are built up from $[TiO_6]$ octahedra and $[PO_4]$ tetrahedra which are linked by corner sharing along the c-axis. M^{2+}= Mn^{2+}, Co^{2+}, Ni^{2+}cations are located in half of the antiprism M_1 sites and are orderly. The corresponding titanium phosphates $Li_{0.5}M_{0.25}Ti_2(PO_4)_3$ (M= Mn, Co, Ni) photocatalyst were then characterized by means of X-ray diffraction (XRD), FT-IR, Raman and diffused reflectance spectroscopy, (SEM), MEB. The photocatalytic activity of $Li_{0.5}M_{0.25}Ti_2(PO_4)_3$ (M= Mn, Co, Ni) was investigated by testing the photo-degradation of 4-nitrophenol in aqueous solution under visible light irradiation with the assistance of appropriate amount of H_2O_2. The results indicated that the photo-degradation of 4-nitrophenol was much enhanced compared with the bare TiO_2.*

Keywords: *Titanium Phosphates, Photocatalysis; Photocatalyticdegradation, 4-Nitrophenol.*

1. INTRODUCTION

A typical group of organic pollutants is the phenols and its derivative such as 4-Nitrophenol (4-NP). These are important environmental pollutants generated from pesticides, herbicides, paints, leathers, and the textile and paper manufacturing industries [1-3]. Most of those pollutants can remain in the environment for long periods and cause serious environmental problems since they have high toxicity and poor biodegradability. These contaminants have led to the priority pollutants by the United States Environmental Protection Agency (USEPA) due to their harmful effect to organisms at low concentration [4, 5]. Thus, the efficient removal of phenol and its derivatives from wastewater has attracted extensive attention. The conventional methods for removing phenolic pollutants from water such as activated carbon adsorption, microbial degradation, solvent extraction and chemical oxidation are frequently used [6,7]. The high cost of activated carbon, solvent extraction and oxidation treatments has stimulated interest to use cheaper raw materials. Titanium dioxide (TiO_2) is generally considered to be the best photo catalyst and has the ability to de-toxificate water from a number of organic pollutants [8]. TiO_2 is of great interest because of photo catalytically stable for his favorable band gap energy (TiO_2: ~3.1 eV), non-toxic nature, low cost material, chemically and biologically inert, easy to produce and to use without risks to environments and humans [9]. TiO_2 exhibits high adsorption ability to phenolic pollutants, corresponding with good quality photocatalytic efficiency. However, shortcoming of using TiO_2 in photocatalytic processes is its rapid aggregation in a suspension resulting in decrease of effective surface area in addition to recombination of generated electron–hole pairs. This disadvantage of TiO_2 results in low catalytic efficiency.

Various methods are documented to improve photocatalytic efficiency of TiO_2[10-12]The dispersion of TiO_2 with supports has become attractive because of supports' adsorption capability which results into composite photocatalyst. TiO_2 with supports or co-sorbent offers high specific surface area, which helps in more effective adsorption than TiO_2 alone [13-15]. The synergy between TiO_2 particle and the support enhances the degradation which is attributed to reduction in the electron–hole recombination reaction on the surface [16].

Recently Bismuth phosphate ($BiPO_4$) with a non-metal oxy-acid structure has shown excellent photocatalytic activity for methylene blue degradation and mineralization [17]and its efficiency is double than that of TiO_2. The excellent photocatalytic activity of $BiPO_4$ originates in the inductive effect of PO_4^{3-} , since it is prone to separate electron and hole. The absorption edge of $BiPO_4$ occurs at about 322 nm, which is equivalent to band gap energy of 3.85 eV approximately.

In this work, new titanium metal phosphates $Li_{0.5}M_{0.25}Ti_2(PO_4)_3$ with M=Mn, Co and Ni were synthesized by solid state methods. The samples have been characterized by X-ray diffractometry (XRD), Infrared and Raman spectroscopy, diffuse reflectance spectroscopy; scanning electron microscopy (SEM), MEB, structural and identification are explained by XRD. Morphology of materials was investigated by SEM. Vibrational spectroscopic study with Infrared and Raman spectroscopic data confirms the formation and structure of the materials. The photo activity of the samples was tested for 4-nitrophenol photodegradation in aqueous medium chosen as a probe reaction. Aim of this study is investigation of the applicability of these titanium phosphates for the minimization of the 4-nitrophenol content in aqueous solutions under visible light irradiation. The great stability of the tetrahedral oxyanions $(PO_4)^{3-}$ gives phosphates a remarkable structural diversity in the case of monophosphates (Nasicon, Alluaudite, and Langbeinite). In general, these structures have the same type of framework and different types of cavities for accommodating cations. Physical and chemical properties of all these types of monophosphates depend on their structure resulting from the Coulomb attraction between independent cations and oxyanions.

2. EXPERIMENTAL

2.1. The Preparation of $Li_{0.5}M_{0.25}Ti_2(PO_4)_3$ (M=Mn, Co and Ni)

$Li_{0.5}M_{0.25}Ti_2(PO_4)_3$ (M=Mn, Co and Ni) materials are synthesized by solid state reaction method. Stoichiometric amounts of Li_2CO_3, TiO_2, MO (M=Mn, Co and Ni) and $(NH_4)_2HPO_4$ for these composition are finely ground in an agate mortar for about four hours to obtain an homogeneous mixture. The powder samples are then calcined at 800°C for 4h with heating rate of 5°C per minute and then at 1050°C for 2h.

2.2. Structural Characterization

2.2.1. X-ray diffraction

Phase identification of calcined powders are performed on XRD Rigaku diffractometer equipped with CuKα radiation λ=1.5406A from 20° to 80°.The accelerating voltage and current used were 40 kV and 26 mA, respectively.

2.2.2. Infrared spectroscopy

Infrared transmittance spectra were measured at room temperature in KBr disc using the FTIR spectra of crystals recorded on Perkin–Elmer Fourier transform spectrometer 1700 in the frequency range 400–4000 cm^{-1}.

2.2.3. *Raman spectroscopy*

Raman spectroscopy was used by means of a Jasco FT-Raman 6000 spectrometer with a Nd/YAG laser excitation at 1064 nm and a spectral resolution of 4 cm^{-1}. The Raman spectra were collected by rotating the sample stage relative to the fixed laser beam.

2.2.4. SEM micrographs

Scanning electron microscopy (SEM) was carried out on a Zeiss Evo 40 scanning electron microscope machine at different magnifications, from 4000 to 20,000 on sintered specimen samples of $Li_{0.5}Ni_{0.25}Ti_2(PO_4)_3$ (M = Mn, Co and Ni).

2.2.5. UV-Vis measurements

Absorption spectra were recorded in the range 200–800 nm by using a Varian CARY 100 Scan UV-vis spectrophotometer.

2.3. Photodegradation Measurements

The set-up used for the photocatalytic experiments consists of a 500 ml glass Pyrex reactor containing 4-NP solution/photocatalyst suspension placed in the center of a wood box and irradiated from the top with a 300 W UV-visible lamp (SANOLUX HRC) emitting five main peak sat the wavelengths 364.65, 404.59, 435.37, 545.38 and 578.22 nm. The lamp was housed in the upper window of the box at 14 cm distance from the reactor, and the radiant flux measured by a DELTA OHM Photo-Radiometer HD 9221, equipped with a sensor LP 9221 PHOT, was 340 W/m^2 in the 200–950 nm range. Oxygenation was ensured by bubbling air in the suspension during the experiments. The novel photo catalysts based on titanium phosphate structure have been used to test the degradation of 4-NP as a probe pollutant molecule. The degradation process of 4-NP has been evaluated as the ratio of the concentrations C_t/C_0 *vs* time. C_t and C_0 were calculated measuring the absorbance values A_t and A_0 of 4-nitrophenol at 317 nm at time t and at the initial time t_0, respectively, by means of a UV-vis spectrophotometer.

3. RESULTS AND DISCUSSION

3.1. Crystal Structure and Morphology Characterization

The room temperature powders X-ray diffractograms of all the three compounds are shown in Fig. 1. It is observed from these figures that all compounds forms single phase with no detectable impurity. These patterns are similar to that of sodium and titanium analogues of same Nasicon framework reported earlier [18-20]. The unit cell parameters are calculated by using least square refinement method. The lattice parameters thus obtained for all the compounds are presented in Table 1, along with other similar Nasicon compositions for a comparison. All these compositions crystallize in rhombohedral lattice with space group R-3c. A small variation in the lattice parameters is observed which is attributed to the variation of the size of divalent metal ion. The powder patterns of $Li_{0.50}M_{0.25}Ti_2(PO_4)_3$ (M=Mn, Co, Ni) phases clearly showed the Nasicon structure type. However, the presence of reflections $h\bar{h}0l$ with l = 2n + 1 induced the space group $R\bar{3}$. Unit-cell parameter variation with the ionic radii of M^{2+} (M^{2+}=Mn^{2+}, Co^{2+}, Ni^{2+}) ions showed a slight contraction along the *a* axis and expansion along the *c* axis. The Rietveld method [21] using the FULLPROF program [22], was used to refine the XRD powder pattern of $Li_{0.50}M_{0.25}Ti_2(PO_4)_3$ (M=Mn, Co, Ni) phases. In the first attempt, the coordinates of the $Co_{0.5}Ti_2(PO_4)_3$ [23] atoms were taken as starting point. Refinements in the space group $R\bar{3}c$(N°.167), lead to large agreement factors and inter-atomic distances without physical meaning. The second attempt performed with space group R^{32}, as in $Co_{0.5}Ti_2(PO_4)_3$ [24]. Both refinements lead to a rejection of an occupation of site M_2 by any atoms. Next, The Rietveld refinements were performed in the $R\bar{3}$ space group with the initial coordinates of $Mn_{0.5}Ti_2(PO_4)_3$ [18] gave better results. An assignment of (M=Mn, Co, Ni), Ti and O to two series of independent sites was chosen. Refinement led to acceptable agreement factors with an occupation factor of one site equal to zero and a quite high thermal displacement factor. Figures 2, 3 and 4 show the comparison between experimental and calculated patterns. Final atomic coordinates and thermal displacement factors are gathered with occupation assignments in Table 2. Selected inter-atomic distances are displayed in Table 3.

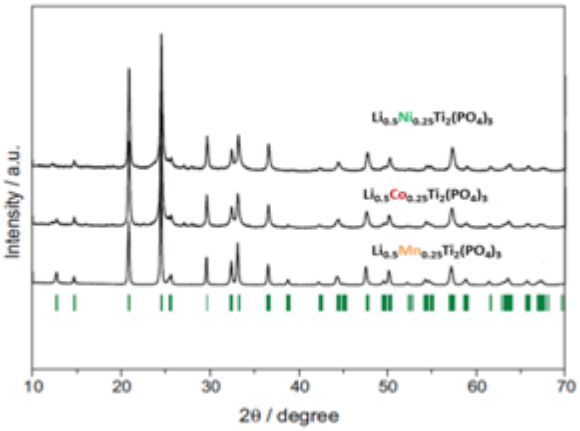

Figure1. *XRD patterns of $Li_{0.5}M_{0.25}Ti_2(PO_4)_3$(M=Mn, Co, Ni) sintered powders.*

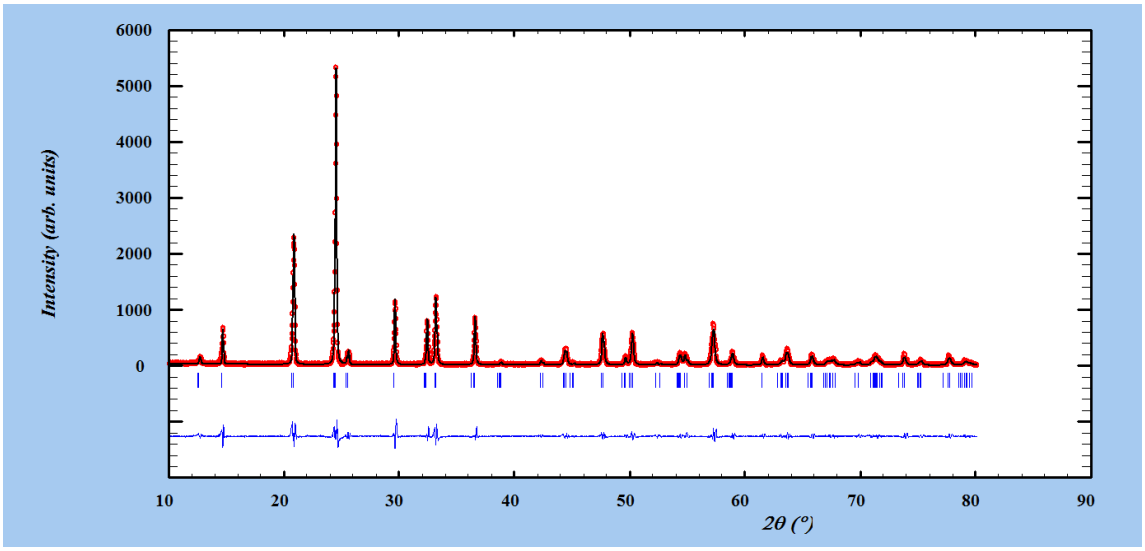

Figure2. *Final observed (••••••) calculated (—) and difference X-ray diffraction patterns for* $Li_{0.5}Mn_{0.25}Ti_2(PO_4)_3$.

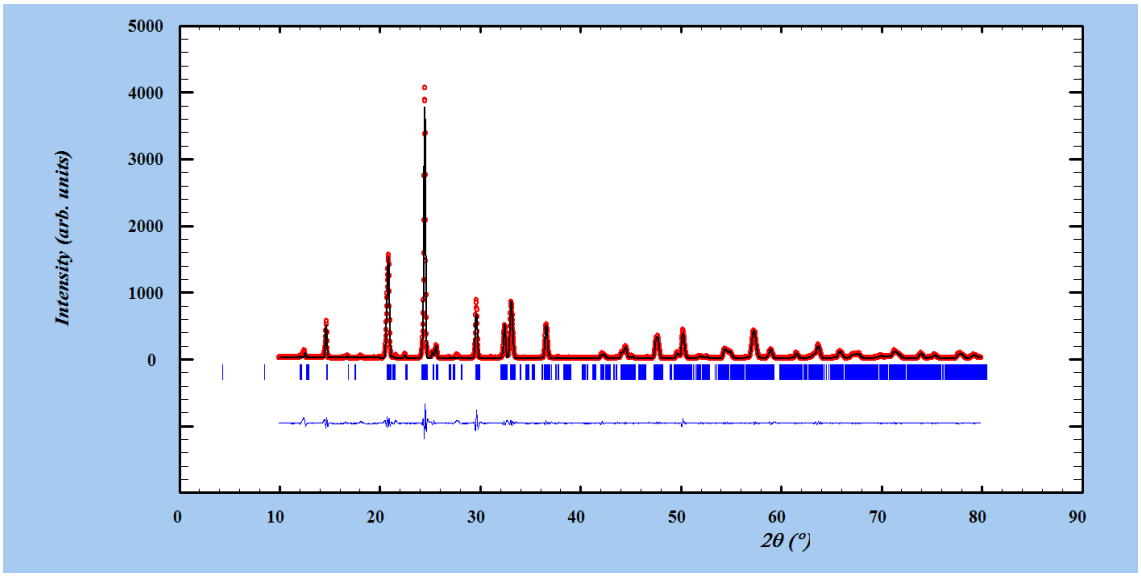

Figure4. *Final observed (••••••) calculated (—) and difference X-ray diffraction patterns for* $Li_{0.5}Co_{0.25}Ti_2(PO_4)_3$.

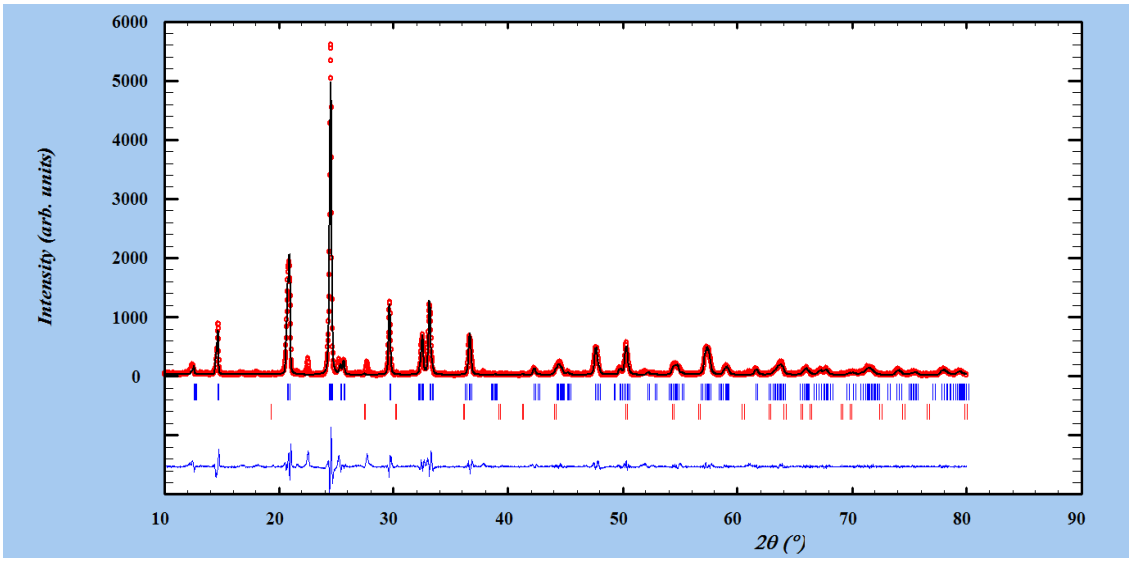

Figure3. *Final observed (••••••) calculated (—) and difference X-ray diffraction patterns for* $Li_{0.5}Ni_{0.25}Ti_2(PO_4)_3$.

Table1. *Composition, lattice parameters and densities of $Li_{0.5}M_{0.25}Ti_2(PO_4)_3$ (M = Mn, Co, and Ni).*

Compound	G.S	a(Å)	c(Å)	Reference
$Li_{0.5}Mn_{0.25}Ti_2(PO_4)_3$	R -3	8.5028(2)	20.9520(13)	Present work
$Li_{0.5}Co_{0.25}Ti_2(PO_4)_3$	R -3	8.49000(2)	21.024849	Present work
$Li_{0.5}Ni_{0.25}Ti_2(PO_4)_3$	R -3	8.5025(2)	20.9472(13)	Present work
$Mn_{0.5}Ti_2(PO_4)_3$	R -3	8.51(1)	21.087(2)	[18]
$Co_{0.5}Ti_2(PO_4)_3$	R -3c	8.510(1)	21.033(2)	[23,24]
$LiTi_2(PO_4)_3$	R-3c	8.512	20.858	JCPDS N°.35-0754

Table2. *Atomic coordinates and equivalent isotropic displacement parameters ($Å^2$) for $Li_{0.5}M_{0.25}Ti_2(PO_4)_3$ (M = Mn, Co, Ni).*

Phase	Atom	X	Y	Z
$Li_{0.5}Mn_{0.25}Ti_2(PO_4)_3$	Ti1	0.00000	0.00000	0.14650(4)
	Mn1	0.00000	0.00000	0.00000
	Ti2	-0.66667	-0.33333	0.30330 (5)
	P1	-0.29240(11)	-0.28500 (1)	0.25000 (6)
	O1	-0.02700(3)	-0.19400 (3)	0.07960 (9)
	O2	-0.18400(2)	-0.18800 (3)	0.19370 (9)
	O3	-0.48100(3)	-0.31000 (3)	0.25360 (7)
	O4	-0.17500(3)	-0.20400 (2)	0.31190(9)
	Li1	-0.66667	-0.33333	0.16667
$Li_{0.5}Co_{0.25}Ti_2(PO_4)_3$	Ti1	0.00000	0.00000	0.14630(4)
	Co1	0.00000	0.00000	0.00000
	Ti2	-0.66667	-0.33333	0.30320 (5)
	P1	-0.29210 (11)	-0.28560 (1)	0.25010 (6)
	O1	-0.02800 (3)	-0.19500 (3)	0.07970 (8)
	O2	-0.18300 (2)	-0.18800 (3)	0.19370 (9)
	O3	-0.48200(3)	-0.31000 (3)	0.25390 (7)
	O4	-0.17400 (3)	0.20300 (2)	-0.31170 (9)
	Li1	-0.66667	-0.33333	0.16667
$Li_{0.5}Ni_{0.25}Ti_2(PO_4)_3$	Ti1	0.00000	0.00000	0.14630 (4)
	Ni1	0.00000	0.00000	0.00000
	Ti2	-0.66667	-0.33333	0.30320 (5)
	P1	-0.29000(10)	-0.28570 (1)	0.25020 (6)
	O1	-0.02800(3)	-0.19500 (3)	0.07970 (8)
	O2	-0.18300 (2)	-0.18800 (3)	0.19360 (8)
	O3	-0.48200 (3)	-0.31000 (3)	0.25400 (7)
	O4	-0.17300(3)	-0.20300 (2)	0.31150 (8)
	Li	-0.66667	-0.33333	0.16667

Table3. *Bond distances (Å) for $Li_{0.5}M_{0.25}Ti_2(PO_4)_3$(M = Mn, Co, Ni).*

Bond distances (Å) for $Li_{0.5}Mn_{0.25}Ti_2(PO_4)_3$		**Bond distances (Å) for $Li_{0.5}C_{0.25}Ti_2(PO_4)_3$**		**Bond distances (Å) for $Li_{0.5}$ $Ni_{0.25}Ti_2(PO_4)_3$**	
Li-O(1)	2.35×6	Li-O(1)	2.35×6	Li-O(1)	2.35×6
Ti(1)-O(1)	2.0912(2) ×3	Ti(1)-O(1)	2.09(2) ×3	Ti(1)-O(1)	2.09(2) ×3
Ti(1)-O(2)	1.8638(3) ×3	Ti(1)-O(2)	1.86(3) ×3	Ti(1)-O(2)	1.86(3) ×3
Ti(2)-O(1)	1.82(2)×3	Ti(2)-O(1)	1.81(2)×3	Ti(2)-O(1)	1.81(2)×3
Ti(2)-O(2)	1.96(2)×3	Ti(2)-O(2)	1.95(2)×3	Ti(2)-O(2)	1.95(2)×3
Co(2)-O(1)	2.28×6	Co(2)-O(1)	2.27993×6	Ni(2)-O(1)	2.28446 ×6
P-O(1)	1.54(3)	P-O(1)	1.54(3)	P(2)-O(1)	1.47(3)
P-O(2)	1.47(2)	P-O(2)	1.47(2)	P(2)-O(2)	1.51(2)
P-O(3)	1.51(3)	P-O(3)	1.51(3)	P(2)-O(3)	1.51(3)
P-O(4)	1.57(2)	P-O(4)	1.57(2)	P(2)-O(4)	1.57(2)

$Li_{0.50}M_{0.25}Ti_2(PO_4)_3$ (M=Mn, Co, Ni) has a Nasicon-type structure similar to that of the $Mn_{0.5}Ti_2(PO_4)_3$ phase [18]. The crystallographic formula can be written as is $[Li_{0.50}]_{M2}[M_{0.25}]_{M1}[Ti_2]_A(PO_4)_3$(M=Mn, Co, Ni). The structure consists of a three-dimensional framework of $[PO_4]$ tetrahedra and $[TiO_6]$ octahedra sharing corners Figures 7, 8. The $[PO_4]$ tetrahedra are regular with a weak dispersion of the O–P–O angles between 101.07(65)° and 115.94(62)°, which is about the ideal value of 109.45°. The <P–O> distance =1.5225(7) Å, which is typical of monophosphate, is close to the distances found in $Mn_{0.50}Ti_2(PO_4)_3$ (<P–O> = 1.562(6) Å). As emphasized before, M=Mn, Co, Ni ions occupy the M_I sites, in the 3a sites.

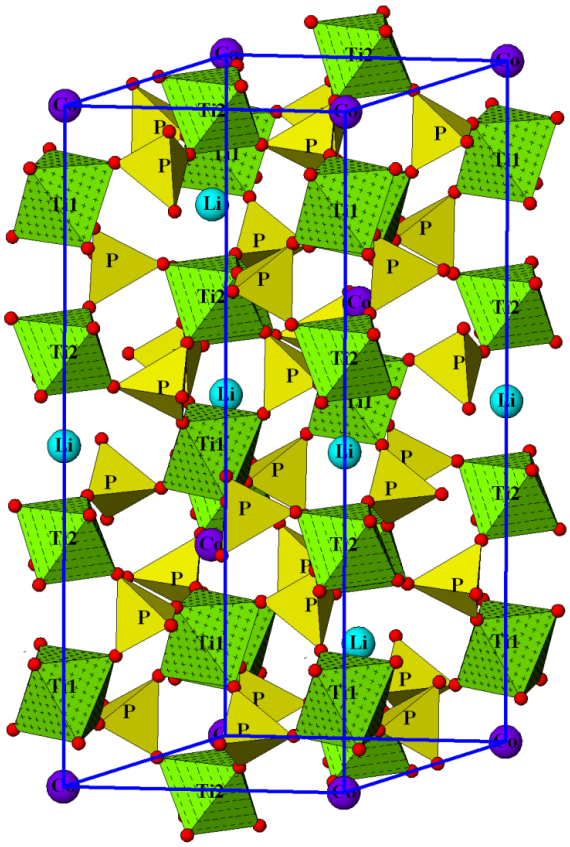

Figure5. A polyhedral view of framework as projected in the (b, c) plane of $Li_{0.5}M_{0.25}Ti_2(PO_4)_3$ (M=Mn, Co, Ni).

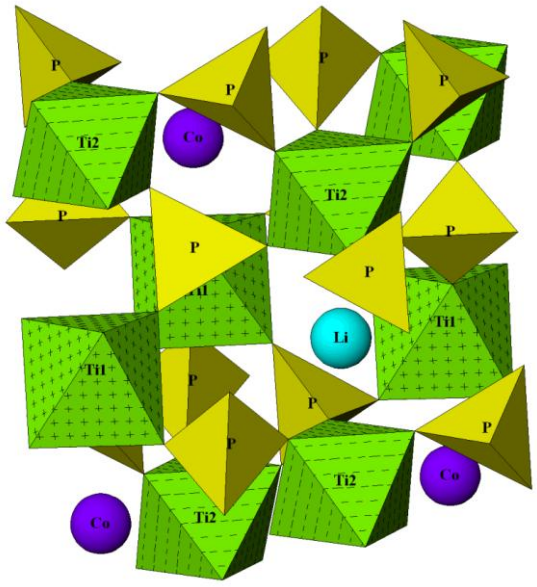

Figure6. *Crystal structure of $Li_{0.5}M_{0.25}Ti_2(PO_4)_3$ (M=Mn, Co, Ni).*

3.2. IR Spectroscopy

Infrared spectra of the compounds $Li_{0.5}M_{0.25}Ti_2(PO_4)_3$ (M = Mn, Co, and Ni) are shown in Figure 7 In the spectra two main regions can be identified in the range 1300–400 cm^{-1} which are attributed to the phosphate unit:

(1) The bands between 1250 and 900 cm^{-1} are ascribed to the stretching vibrations of the PO_4^{3-} unit (ν_1 and ν_3 modes)

(2) The bands between 650 and 400 cm^{-1} are due to the deformation of the O–P–O angle (ν_2 and ν_4 modes).

The ν_3 mode is very sensitive to any phosphate distortion caused by the polarizing effect of the neighbouring metal ions in the crystal structure [25]. The broad bands and complexity of these spectra indicate that the phosphate group is highly distorted, and the symmetry of the PO_4^{3-}group reduced to D_{3h} from the Td symmetry of the isolated ion. The dimension and the charge of the metal ions contained in the ribbons of the crystalline structure influence the degree of distortion of the PO_4^{3-} unit and consequently the strength of the P–O bonds. Table 4 shows the frequencies of the bands as a function of the metal ion (M=Ti^{4+}, and M^{2+} = Mn^{2+}, Co^{2+}, and Ni^{2+}). The bands ν_2 and ν_4 assigned to O–P–O bending modes.

Due to the instrumental constraints the spectra could not be recorded below 400 cm^{-1} and hence the corresponding assignments could not be made.

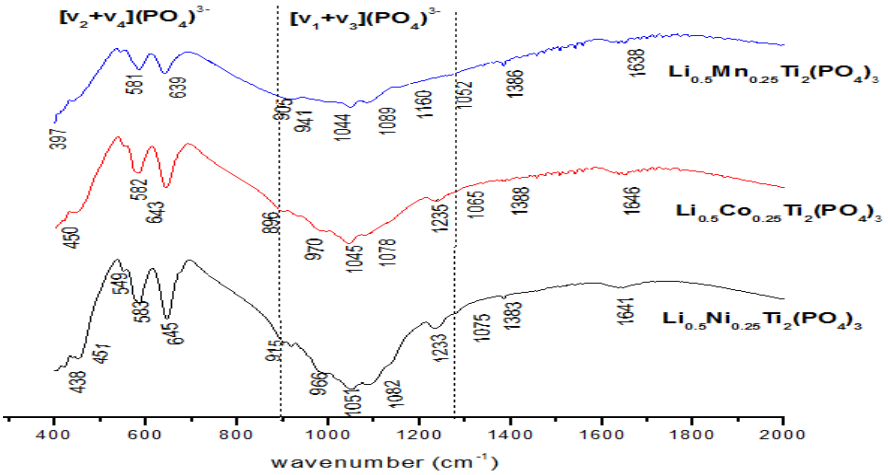

Figure7. *Infrared spectra of Li0.5M0.25Ti2(PO4)3(M = Mn, Co, Ni).*

Table4. *IR data for $Li_{0.5}M_{0.25}Ti_2(PO_4)_3$ (M = Mn, Co, and Ni), the band positions and assignments are in cm^{-1}.*

Compound	ν_3, ν_{as}(P-O)	ν_1, ν_s(P-O)	ν_4, δ(O-P-O)	ν_2 (O-P-O)
$Li_{0.5}Mn_{0.25}Ti_2(PO_4)_3$	1243-1000 cm^{-1}	1000-905 cm^{-1}	674-534 cm^{-1}	457-418 cm^{-1}
$Li_{0.5}Co_{0.25}Ti_2(PO_4)_3$	1267-1000 cm^{-1}	1000-896 cm^{-1}	671-537 cm^{-1}	461-421 cm^{-1}
$Li_{0.5}Ni_{0.25}Ti_2(PO_4)_3$	1275-1000 cm^{-1}	1000-915 cm^{-1}	670-540 cm^{-1}	460–425 cm^{-1}

3.3. Raman Spectroscopy

Vibrational spectra have been recorded for the three compound $Li_{0.50}Mn_{0.25}Ti_2(PO_4)_3$, $Li_{0.5}Co_{0.25}Ti_2(PO_4)_3$ and $Li_{0.50}Ni_{0.25}Ti_2(PO_4)_3$. Figure 8 shows their Raman spectra. The high frequency part (900– 1200 cm^{-1}) of these spectra corresponds to the stretching vibrations of the PO_4 tetrahedra and exhibits six peaks. The peaks observed between 700 and 400 cm^{-1} are assigned to the P–O bending vibrations. The peaks situated below 400 cm^{-1} are attributed to the external modes.

Table5. *Spectral data (cm^{-1}) for $Li_{0.5}M_{0.25}Ti_2(PO_4)_3$ (M = Mn, Co, and Ni), the band positions*

Compound	stretching vibrations	bending vibrations
$Li_{0.50}Mn_{0.25}Ti_2(PO_4)_3$	944, 993, 1011, 1075, 1090	450, 546, 605, 655, 699
$Li_{0.50}Co_{0.25}Ti_2(PO_4)_3$	905, 938, 995, 1008, 1073, 1097	434, 448, 463
$Li_{0.50}Ni_{0.25}Ti_2(PO_4)_3$	899, 920, 1008, 1070, 1090	436, 456, 471

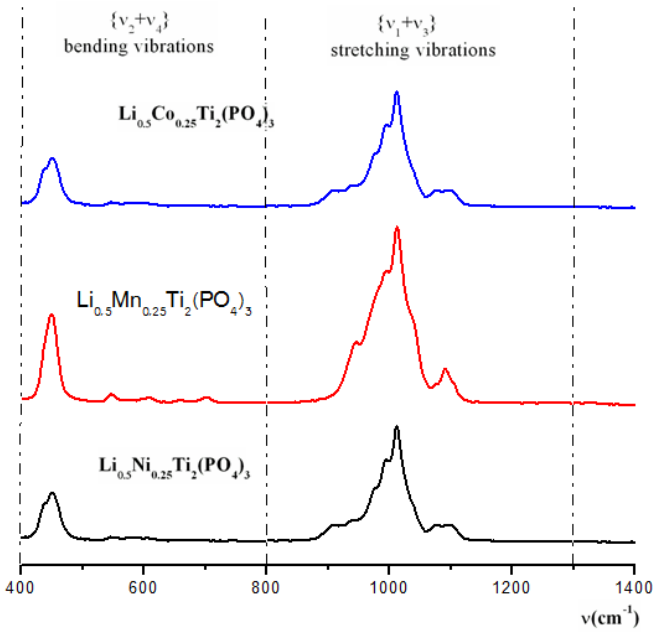

Figure8. *Raman spectra of* $Li_{0.5}M_{0.25}Ti_2(PO_4)_3$*(M = Mn, Co, Ni).*

3.4. SEM characterization

The particle morphologies were examined by SEM Figure 9 shows the SEM micrographs of $Li_{0.5}Mn_{0.25}Ti_2(PO_4)_3$. All observed peaks were assigned to the elements present in $Li_{0.5}Ni_{0.25}Ti_2(PO_4)_3$ compounds.

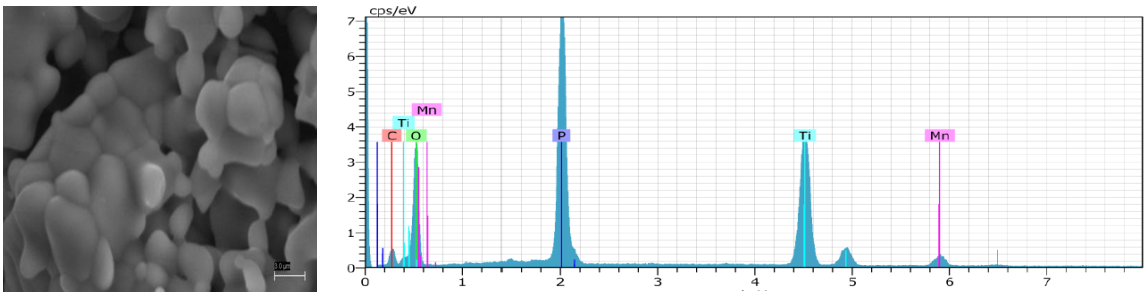

(a)

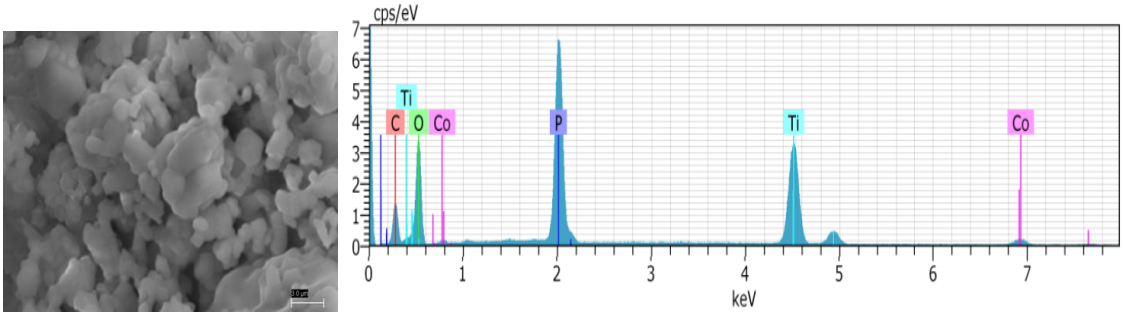

(b)

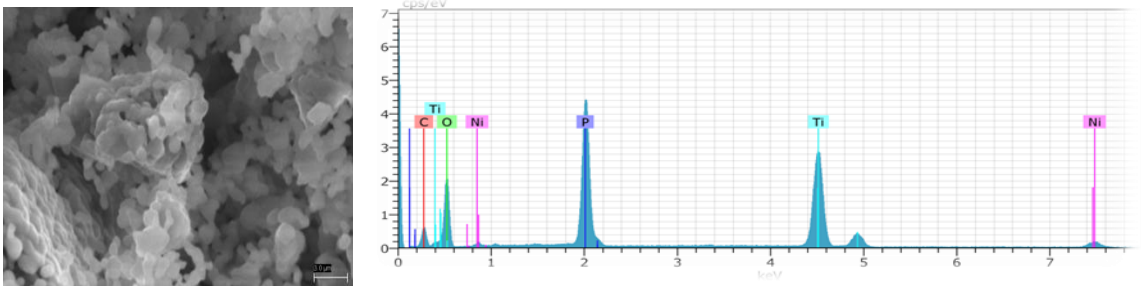

(c)

Figure9. SEM micrographs of (a) $Li_{0.5}Mn_{0.25}Ti_2(PO_4)_3$, (b)$Li_{0.5}Co_{0.25}Ti_2(PO_4)_3$ and (c) $Li_{0.5}Ni_{0.25}Ti_2(PO_4)_3$.

3.5. Optical Properties $Li_{0.5}Ni_{0.25}Ti_2(PO_4)_3$

The UV–vis spectrum of the titanium phosphate $Li_{0.5}Ni_{0.25}Ti_2(PO_4)_3$ showed a very strong absorption band in the 250-500 nm wavelength region (Fig. 10). This band is similar to that of rutile and can be attributed to the octahedral coordination of Ti in the network. The strong absorption band observed in ultraviolet region at 368 nm (27175 cm^{-1}) is attributed to the electronic $O^{2-}(2p)$ to $Ti^{4+}(3d)$ charge transfer:

$$O^{2-}(2p^6) + Ti^{4+}(3d^0) \rightarrow O^{-}(2p^5) + Ti^{3+}(3d^1)$$

The value of the absorption threshold Eg (eV) is 3.37 eV. The value of the optical energy gap is greater than that of TiO_2 rutile (Eg = 3.00 eV) (24191 cm^{-1}) due to the presence of the covalent P–O bonds around Ti^{4+}.

The other bands occurring in the visible and infrared domains might be attributed to d–d transitions of Ni^{2+} in octahedral site. Three spin allowed transition from the $^3A_{2g}(F)$ ground state to the $^3T_{2g}(F)$, $^3T_{1g}(F)$,$^3T_{1g}(P)$ excited states.

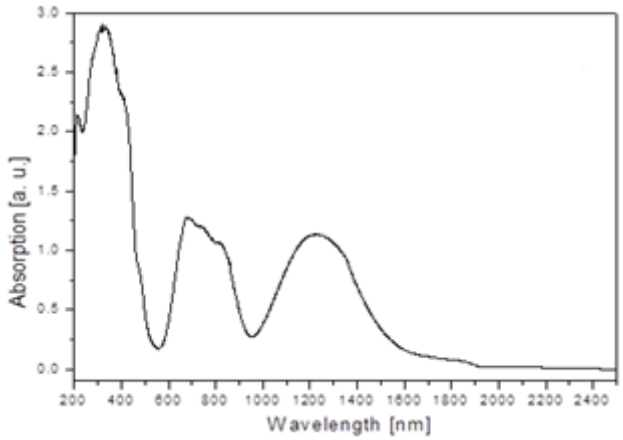

Figure10. *Absorption spectra of $Li_{0.5}Ni_{0.25}Ti_2(PO_4)_3$.*

3.6. Photocatalytic Degradation of 4-Nitrophenol

For the first time, in this work, has been compared the photocatalytic activity of novel polycrystalline Nasicon-type phosphates $Li_{0.5}Ni_{0.25}Ti_2(PO_4)_3$, $Li_{0.5}Co_{0.25}Ti_2(PO_4)_3$ and $Li_{0.5}Mn_{0.25}Ti_2(PO_4)_3$ in order to perform the degradation of 4-nitrophenol (4-NP) in aqueous suspension under UV-visible light irradiation in the presence of H_2O_2. Their photocatalytic activity was also compared with that of pristine TiO_2 in pure anatase phase by using processes conditions chosen by taking into account our previous work [26].

In a typical experiment the photodegradation of 20mg·L^{-1} solution of 4-NP was carried out at the initial value of in the presence of mM, catalyst amount = 0.08g·L^{-1} under air atmosphere in a 300mL batch photoreactor. Sanolux HRC 300W UV-visible lamp was used as irradiation system. The emission spectrum of the radiation source has been shown in Figure 11.

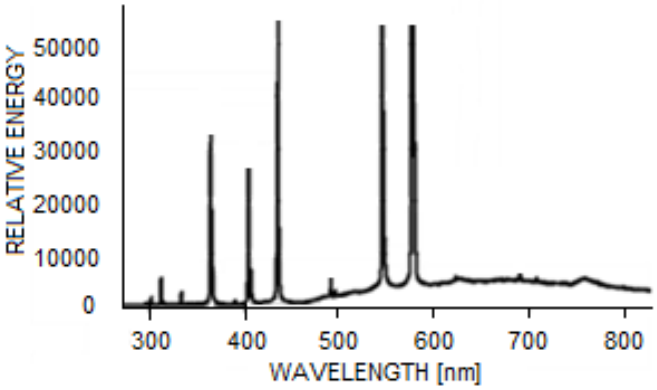

Figure11. *Absorption spectrum of the Sanolux HRC 300 W UV-visible lamp.*

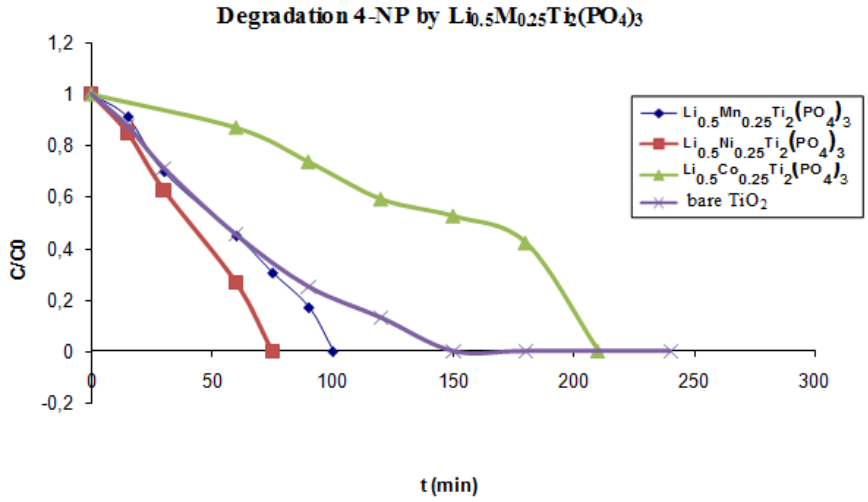

Figure12. *Photodegradation of 4-NP vs irradiation in the presence of $Li_{0.5}M_{0.25}Ti_2(PO_4)_3$(M = Mn, Co, Ni) and bare TiO_2.*

As shown in Figure 12 $Li_{0.5}Ni_{0.25}Ti_2(PO_4)_3$, $Li_{0.5}Co_{0.25}Ti_2(PO_4)_3$ and $Li_{0.5}Mn_{0.25}Ti_2(PO_4)_3$ showed good activities by carrying out the degradation of 4-NP as probe reaction in aqueous suspension under heterogeneous photo-Fenton-type reactions by using UV-visible light. Interestingly, it can be noticed that the photodegradation of 4-NP decreases in following order: $Li_{0.5}Ni_{0.25}Ti_2(PO_4)_3$> $Li_{0.5}Mn_{0.25}Ti_2(PO_4)_3$>$TiO_2$>$Li_{0.5}Co_{0.25}Ti_2(PO_4)_3$.

In particular, $Li_{0.5}Ni_{0.25}Ti_2(PO_4)_3$ and $Li_{0.5}Mn_{0.25}Ti_2(PO_4)_3$showed the best activity in fact 4-NP disappeared completely respectively within 75 and 100 minutes of irradiation time.

Negligible photoactivity was observed for all of the samples when carried out under dark. Selected data concerning processes carried out with or without the presence of $Li_{0.5}Ni_{0.25}Ti_2(PO_4)_3$ (Fig. 13) suggested that the irradiated photocatalyst, together with presence of H_2O_2, is essential for inducing the photodegradation of 4-NP processes.

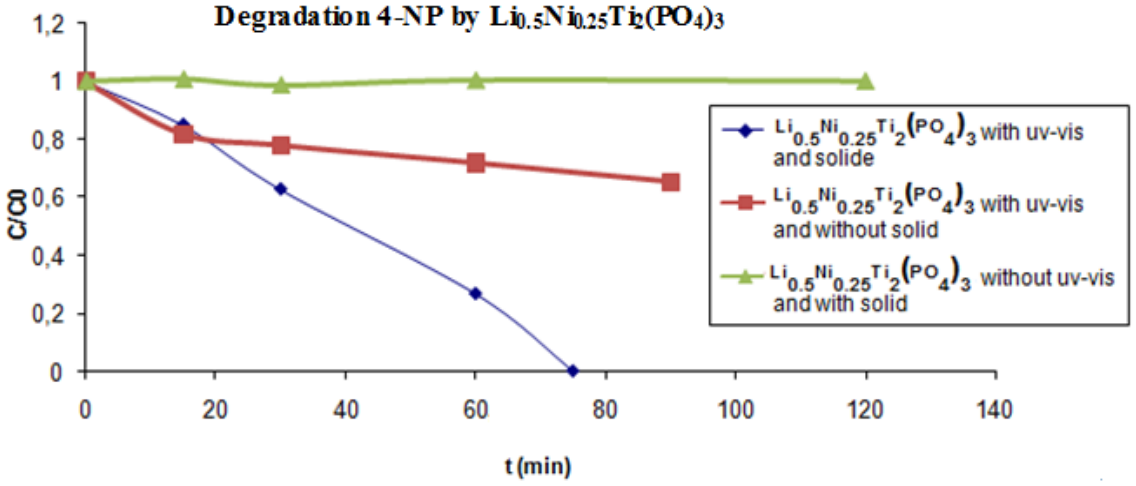

Figure13. *Degradation of 4-NP catalyzed by $Li_{0.5}Ni_{0.25}Ti_2(PO_4)_3$ under different process conditions.*

The photo stability and the reusability of the photo catalysts are important parameters for practical application. In this work we have observed that all the composites, freshly prepared, can be recycled at least three times without any appreciable decrease of photo activity.

The nature of the mechanism involved in the Nasicon-type catalyzed degradation of 4-NP in the presence of H_2O_2 is actually not so clear and it seems that a wide range of mechanism types are implicated. However, the presence of Me^{2+} ions (Me^{2+}= Ni^{2+}, Mn^{2+} and Co^{2+}) produce a beneficial effect on the whole process by involving an increased amount of OH· specie produced by a heterogeneous photo Fenton-like mechanism [26] which could be related to the key steps shown in the following equations (1, 2).

$$Me^{+2} + e^- \rightarrow Me^{+1} \quad (1)$$

$$H_2O_2 + Me^{+1} \rightarrow OH\cdot + OH^- + Me^{+2} \quad (2)$$

4. CONCLUSIONS

In this work we have demonstrated that Nasicon-type phosphates can catalyze the degradation of 4-NP under UV-Vis light irradiation in the presence of hydrogen peroxide. In particular, $Li_{0.5}Ni_{0.25}Ti_2(PO_4)_3$ and $Li_{0.5}Mn_{0.25}Ti_2(PO_4)_3$ were found more efficient than $Li_{0.5}Co_{0.25}Ti_2(PO_4)_3$ or bare TiO_2 in pure anatase phase.

REFERENCES

[1]. M. Kulkarni and A. Chaudhari, "Microbial remediation of nitro-aromatic compounds: An overview," *Journal of Environmental Management*, vol. 85, pp. 496-512, 2007.

[2]. J. C. Spain and D. T. Gibson, "Pathway for Biodegradation of p-Nitrophenol in a Moraxella species," *Applied and Environmental Microbiology*, vol. 57, pp. 812-819, 1991.

[3]. G. R. Chaudhry, A. N. Ali, W. B. Wheeler, "Isolation of a methyl parathion-degrading Pseudomonas sp. that possesses DNA homologous to the opd gene from a Flavobacterium sp.," *Applied and Environmental Microbiology*, vol. 54(2), pp. 288-293, 1988.

[4]. D. Errampalli, O. Tresse, H. Lee, J. T. Trevors, "Bacterial survival and mineralization of p-nitrophenol in soil by green fluorescent protein-marked Moraxella sp. G21 encapsulated cells,"*FEMS Microbiology Ecology*, vol. 30, pp. 229-236, 1999.

[5]. G. E. Parris, "Environmental and metabolic transformation of primary aromatic amines and related compounds," *Residue Revue*, vol. 76, pp. 1-30, 1980.

[6]. S.Muhammad, P. R.Shukla, M. O.Tadé, S. Wang, "Heterogeneous activation of peroxymonosulphate by supported ruthenium catalysts for phenol degradation in water," *Journal of Hazardous Materials*, vol. 215-216, pp. 183-190, 2012.

[7]. Z.Zeng, H.Zou, X.Li, B. Sun, J.Chen, L.Shao, "Ozonation of phenol with O_3/Fe(II) in acidic environment in a rotating packed bed," *Industrial & Engineering Chemistry Research*, vol. 51(31),pp. 10509–10516, 2012.

[8]. A. Mills and S. K. Lee,"A web-based overview of semiconductor photochemistry-based current commercial applications," *Journal of Photochemistry and Photobiology A: Chemistry*, vol. 152, pp. 233-247, 2002.

[9]. A. Mills, G. Hill, S. Bhopal, I. P. Parkin, and S. A. O'Neil, "Thick titanium dioxide films for semiconductor photocatalysis," *Journal of Photochemistry and Photobiology A: Chemistry*, vol. 160, pp. 185-194, 2003.

[10]. J. C.Yu, L.Zhang, J.Yu, "Rapid synthesis of mesoporous TiO_2 with high photocatalytic activity by ultrasound-induced agglomeration," *New Journal of Chemistry*, vol. 26, pp. 416-420, 2002.

[11]. B.Neppolian, H. C.Choi, S.Sakthivel, B.Arabindoo, V.Murugesan, "Solar/UV-induced photocatalytic degradation of three commercial textile dyes," *Journal Hazardous Materials*, vol. 89, pp. 303-317, 2002.

[12]. C. Y.Kuo and H. Y.Lin, "Effect of Coupled Semiconductor System Treating Aqueous 4-Nitrophenol," *Journal of Environmental Science and Health: Part A*, vol. 39, pp. 2113-2127, 2004.

[13]. C.Anderson, A. J. Bard "An improved photocatalyst ofTiO_2/SiO_2prepared by a sol-gel synthesis," *The Journal of Physical Chemistry*, vol. 99(24),pp. 9882–9885, 1995.

[14]. Anderson C, Bard A J. "Improved photocatalytic activity and characterization of mixed TiO_2/SiO_2 and TiO_2/Al_2O_3materials,"*The Journal of Physical Chemistry B*, vol. 101(14),pp. 2611–2616, 1997.

[15]. T.Torimoto, Y.Okawa, N.Takeda, H.Yoneyama, " Effect of activated carbon content in TiO_2-loaded activated carbon on photodegradation behaviors of dichloromethane," *Journal of Photochemistry and Photobiology A: Chemistry*, vol. 103(1),pp. 153–157, 1997.

[16]. J. M.Lopez Nieto, "Microporous and mesoporous materials with isolated vanadium species as selective catalysts in the gas phase oxidation reactions," *Topics in Catalysis*, vol. 15, pp. 189-194, 2001.

[17]. Y. Zhang, R. Selvaraj, M.Sillanpää, Y. Kim, C. W. Tai, "The influence of operating parameters on heterogeneous photocatalytic mineralization of phenol over BiPO4,"Chemical Engineering Journal, vol. 245, pp. 117–123,2014.

[18]. H. Fakrane, A. Aatiq, M. Lamire, A. El Jazouli, C. Delmas, "Chemical, structural and magnetic studie of Mn0.50Ti2(PO4)3 and its solid solution with NaTi2(PO4)3," Annales de Chimie Sciencedes Materiaux,vol. 23,pp. 81-84, 1998.

[19]. S. Barth, R. Olazcuaga, P. Gravereau, G. Le Flem, P. Hagenmuller,"Mg0.5Ti2(PO4)3 – a new member of the NASICON family with low thermal expansion," Materials Letters, Vol. 16,pp. 96-101, 1993.

[20]. A. VenkateswaraRao, V. Veeraiah, A.V. Prasada Rao, B. Kishore Babu, K.Vijaya Kumar, "Influence of Zr4+ doping on structural, spectroscopic and conductivity studies of lithium titanium phosphate," Ceramics International, vol. 40, pp. 13911-13916,2014.

[21]. H.M. Rietveld, "Line profiles of neutron powder-diffraction peaks for structure refinement,"ActaCrystallographica, vol. 22, pp.151-152, 1967.

[22]. J. Rodriguez-Carvajal, "A Program for Rietveld Refinement and Pattern Matching Analysis," Collected Abstract of Powder Diffraction Meeting, Toulouse, France, p. 127, 1990.

[23]. A. El Bouari, A. El Jazouli, J.M. Dance, G. Le Flem, R. Olazcuaga,"A NewNasicon-Like Phosphate Co0.5Ti2(PO4)3,"Advanced Materials Research, vol.1-2,pp. 173-176, 1994.

[24]. R. Olazcuaga, J.M. Dance, G. Le Flem, J. Derouet, L. Beaury, P. Porcher, A. ElBouari, A. El Jazouli, "A New Nasicon-Type Phosphate Co0.5Ti2(PO4)3: I. Elaboration, Optical and Magnetic Properties," Journal of Solid State Chemistry, vol. 143, pp. 224-229,1999.

[25]. R. Pikl, D. deWaal, A. Aatiq, A. El Jazouli, "Vibrational spectra and factor group analysis of Mn(0.5+x)Ti(2-2x)Cr2x(PO4)3 {0≤x≤0.50},"Vibrational Spectroscopy,vol. 16, pp. 137-143, 1998.

[26]. G. Mele, I. Pio, A. Scarlino, E. Bloise, R. Del sole, L. Palmisano, G. Vasapollo, "New Porphyrin/Fe-Loaded TiO2 Composites as Heterogeneous Photo-Fenton Catalysts for the Efficient Degradation of 4-Nitrophenol," Journal of Catalysts, vol. 2013, pp. 7, 2013.